Science in China Series D: Earth Sciences

Research on the dry intrusion accompanying the low vortex precipitation

YAO XiuPing[1,2,3†], WU GuoXiong[1], ZHAO BingKe[4], YU YuBin[3] & YANG GuiMing[2,5]

[1] LASG, Institute of Atmospheric Physics, Chinese Academy of Sciences, Beijing 100029, China;
[2] Institute of Heavy Rain, China Meteorological Administration, Wuhan 430074, China;
[3] China Meteorological Administration Training Center, Beijing 100081, China;
[4] Shanghai Typhoon Institute of China Meteorological Administration, Shanghai 200030, China;
[5] National Meteorological Center of the China Meteorological Administration, Beijing 100081, China

By employing the 6.7μm satellite vapor cloud images and NCEP/NCAR 1°×1° reanalysis datasets, the characteristics and mechanism of the dry intrusion, as well as its impacts on the low vortex precipitation at the Meiyu front are explored in this paper. It is found that the formation,development and maintenance of the low vortex precipitation at the Meiyu front are closely related to the evolution of the dry intrusion. The dry intrusion is characterized by high potential vorticity (PV), low humidity and cold air. The dry intrusion exhibits as an obvious dark zone on vapor cloud images, an area in which atmospheric relative humidity is lower than 60%. However, the features of the dry intrusion on the vapor images are clearer than that of the humidity field, for the former is the digital vapor cloud images with high temporal and spatial resolution, and it can be used to explore the finer characteristics of the development, evolution and supplement of the intrusion during the development of the low vortex. The dry intrusion impacts accompanying the low vortex precipitation at the Meiyu front come from all levels of the troposphere, with the strongest intrusion located at the upper troposphere. The dry and cold air intrudes the vicinity of the low vortex from the upper isentropic surface to the lower one, slanting eastward from lower to higher level. The low vortex precipitation region is usually situated in front of the dry intrusion where the relative humidity gradient is higher. The research also reveals that the mechanism of the dry intrusion is that the high potential vorticity descends from the upper troposphere to the lower level, therefore, the dry intrusion can be used as an important index of the high PV forcing. To the west of the low vortex precipitation, the upper level northerlies descend across the isentropic surface, then the dry cold advection can trigger the instable development in the mid-low troposphere. The dry intrusion enhances the low vortex precipitation. Meanwhile, because of the good agreement between the high PV at the upper level and the dry intrusion illustrated by the vapor cloud images, the dry intrusion in the vapor cloud images is the direct and clear description of the high PV forcing which provides a new insight in understanding the evolution and development of the practical weather systems. Besides, both the skills of isentropic analysis and potential temperature coordinates system analysis are important to revealing the three-dimension structure of the dry intrusion.

Meiyu front, low vortex precipitation, dry intrusion, mechanisim, vapor image, potential vorticity, relative humidity

It is well known that heavy rainfall during the Meiyu period is among the most important weather processes over China and has brought about increasingly frequent disasters (e.g. 1998 & 2003). Great difficulty still exists for studies on catastrophic weather during Meiyu season

Received April 26, 2006; accepted January 23, 2007
doi: 10.1007/s11430-007-0057-1
†Corresponding author (email: yaoxp@mail.iap.ac.cn)
Supported by the National Natural Science Foundation of China (Grant No. 40205008), Heavy Rain Opening Foundation (Grant No. IHR2005K04) and the National Basic Research Program of China (Grant No.2006CB403601)

although much attention has been paid to the heavy rainfall process and its companying weather systems.

The heavy rainfall during the Meiyu season is usually a result of interaction between warm/moist air and cold/dry air[1]. Previous studies about the weather system such as heavy rainfall or mesoscale cyclone emphasized particularly the ascending motion of moist air and the associated release of latent heat. With the development of remote sensing and detection technology, it is found from satellite images that evolutions of weather systems leading to many disasters always have close relations with dry intrusion processes which manifest as dry slots[2].

Danielsen[3] plotted the three-dimensional structure of dry intrusion flow as far back as the 1960s. Nevertheless, it is only since the 1990s that dry intrusion has been studied in detail (e.g. Browning et al. [2,4−6] and Young et al.[7−9]). Dry intrusion means that flow with high potential vorticity and low moist-bulb potential temperature from tropopause intrudes into the low level[2,5]. Dry intrusion flow manifests as dark area in satellite images of water-vapor[10]. According to the viewpoint of transportation belt, potential instability and corresponding convection occurs easily when dry flow characterized by low moist-bulb potential temperature intrudes into warm transportation flow belt. The interaction between cold/dry and warm/moist transportation flow belts is mainly responsible for the development of cyclone. Young et al.[9] point out that the intrusion of dry/cold air from the tropopause plays a significant role in the rapid deepening of cyclone. Studies of Browning and Golding[2] also prove the importance of dry intrusion. Their analysis about one rapid deepening process of cyclone in England shows that squall lines may emerge and then develop once dry/cold air swiftly intrudes into low level region with strong baroclinicity and superposition on the boundary layer with high moist-bulb potential temperature. In addition, dry intrusion also has close relationship with the development of mesocyclones and occurrence of strong tornadoes[11].

All the above studies suggest that the intrusion of dry/cold air from tropopause into low level baroclinic areas or cyclones is favorable for the development of extra-tropical cyclones or mesocyclones and the emergence of burst cyclones[12].

Ninomiya et al.[13] analyze the large-scale circulation during the Meiyu period. Their results showed that warm ridge and cold trough are the main systems over middle-high latitudes and cold advection behind the cold trough contributes much to the maintenance of Meiyu front. Perturbation from middle latitudes moves into Meiyu front region near cut-off low, leading to more rainfall over strong Meiyu front by inducing ascending motion and cold advection[14]. Tao[1] points out that the intrusion of cold advection behind trough on middle-high troposphere into mesoscale convection system exerts important influence on the strengthening of convective instability and development of cyclones. Activity of cold air along westerly belt is indispensable for the formation of large-scale heavy rainfall over middle latitudes. Thus, the timing, location, direction and intensity of cold air are of importance to the prediction of when and how much heavy rainfall would happen. Wu et al.[15,16] suggest that the development of vertical vorticity induced by slant isentropic surface reacts on the occurrence and evolution of severe rainfall during the Meiyu period. Results of Lu et al.[17] and Yu et al.[18] show that the flow with high potential vorticity from middle-high level of troposphere significantly influences the development of heavy rain. Jiang and Ni[19] diagnose the structure and maintenance mechanism of Meiyu front during one weather process. They find that dry/cold air from the trough over middle-high level of troposphere strengthens the intensity of Meiyu front by intruding into the rear of Meiyu front and boosts the development of mesoscale convection system in front of the Meiyu front by cold convection effect. Huang et al.[20] analyze the track of cold air during the heavy rainfall process over the Yangtze-Huaihe region on 4−6 July, 1991. They point out that the cold air from the northwest encounter the warm air over the Yangtze River, leading to the development of the trough at 500 hPa to the east of the Tibetan Plateau, which is favorable for the development of cyclone along Meiyu front. Yuan et al.[21] showed that one super-heavy rainfall process over South China during June of 1998 came into being and then developed under the impact of cold air with high potential vorticity from a blocking pattern over East Asia. Studies of Shou et al.[22] also indicate the cases are the same to the severe rainfall over the Yangtze-Huaihe region. Gao et al.[23] also analyze the origination of cold air leading to the disturbance of Meiyu front over the middle and lower reaches of the Yangtze River and the effects of cold air on the formation of baroclinic front

area. The study of Rogers et al.[24] about the Atlantic cyclone suggests that temperature advection brought by cold air contributes much to the rapid development of cyclone. Lü et al.[25] diagnose an example of spring Yangtze-Huaihe cyclone, they point out that the warm flow from middle and low level of troposphere and the cold flow from middle and upper level had important impacts on the development of cyclone. Davis[26] discusses the potential vorticity inversion during the formation of cyclone, he finds that the superposition of potential vorticity anomaly areas of high and low level is responsible for the formation and development of cyclone, potential voritcity anomaly at high level is mainly due to advection while that at low level is caused by diabatic heating effect. Rossa et al.[27] investigate the development and extinction of PV-Tower of extra-tropical cyclone from Euler and Lagrange viewpoints. Their study also indicates the effects of overlap of potential vorticity anomaly at different levels on extratropical cyclone.

Generally speaking, the studies of foreign scientists pay more attention to the impacts of dry intrusion from middle and high level on synoptic system while domestic studies in China mainly emphasize the effects of cold air from low level during precipitation processes.

Recent studies[28] indicate that storm rainfall frequency is associated with dry intrusion on condition of the maintenance of warm air at low level. But the evolution of dry intrusion and its effects on heavy rainfall processes during the Meiyu season is still not very clear. Whether dry intrusion in East Asia has the same properties as that in other regions remains to be investigated. Studies about the above problems will enhance the understanding about the characteristics of low vortex along the Meiyu front and the mechanism of the development of heavy rainfall. Thus, these studies may provide more insights for the prediction of heavy rainfall during the Meiyu season.

In this paper, 6.7 μm satellite vapor cloud images and NCEP/NCAR reanalysis datasets with horizontal resolution of 1°×1° are used to study the aforementioned questions. Evolution of low vortex and its accompanying precipitation along the Meiyu front are first analyzed. Then characteristics mechanisms of dry intrusion concurrent with low vortex precipitation are revealed. Finally, 3D structure of dry intrusion and its effects on low vortex precipitation are displayed in this paper.

1 Evolution of low vortex precipitation over Meiyu front

The first heavy rainfall after the beginning of Meiyu period of 2003 occurred during 22—25 June, and the rainfall process during 22—23 June mainly resulted from low vortex. The location, surface pressure and rainfall amount near the low vortex center are shown in Figure 1(a). Precipitation came into being in association with the low vortex which moved eastward, developed into cyclone and then entered the sea. The low vortex first originated from the eastern Sichuan Basin on 12UTC of 21 June, it moved northeastward along the southwestly steering flow to the west of Huanghe-Huaihe region on 06UTC of 22 June, and developed into a cyclone on 18UTC of 22 June. Then the cyclone shifted northeastward to the west of Korea Peninsula on 00UTC of 24 June. It began to weaken after moving into the Sea of Japan on 12UTC of 24 June.

Precipitation accompanying the low vortex mostly occurred during 06—18 UTC of 22 June over the Yangtze-Huaihe region. According to the evolution of low vortex precipitation, the initial stage, developing stage and mature stage may be identified as 06UTC of 22 June, 12UTC of 22 June and 18UTC of 22 June.

Precipitation always occurred near low vortex center during the development process of low vortex (not shown). During that period, low vortex precipitation belt mostly distributed over the Yangtze-Huaihe region in north-east-southwest orientation (shown as Figure 1(b)). There are 3 rainfall centers with precipitation more than 150 mm located over Shangdong, Henan and Hubei provinces respectively. Distribution and evolution of rainfall amount every 6 h (not shown) indicates that the rainfall belt centered at 112.5°E, 33°N with rainfall amount above 40 mm is along the east to west direction. The rainfall belt shifted eastward and enhanced in association with the eastward movement and development of low vortex. The low vortex reached 116°E, 34°N with a more than 60 mm precipitation center on 06UTC of 22 June. It moved eastward to 118°E, 35°N with its accompanying rainfall belt in the northeast-southwest direction and the rainfall center above 60 mm expanded on 12UTC of 22 June. At the same time, another rainfall center more than 80 mm appeared to the southwest of the low vortex. On 18UTC of 22 June, the low vortex reached 120°E, 36°N and its rainfall belt split into two

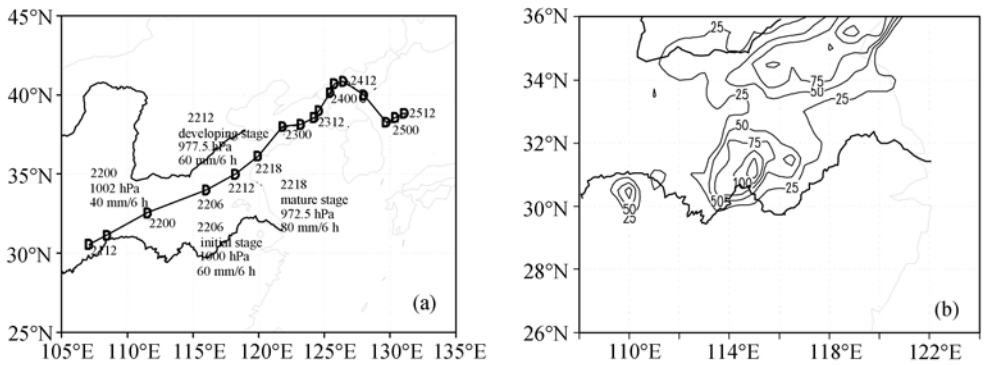

Figure 1 (a) Track of low vortex over the Meiyu front during 21—25 June. D denoting surface low pressure center; numerical numbers such as "2206" representing time 06UTC of 22 June, those such as "1002 hPa" surface pressure of low vortex center and those such as "40 mm/6 h" precipitation of 6 h over low vortex center. (b) Daily precipitation (mm) for the 00UTC of 22 June to 00UTC of 23 June period in 2003.

rainfall centers, one maintained or increased in association with the low vortex and the other intensified to more than 120 mm over Hubei Province. In fact, the latter belonged to the mesoscale convective system developed from the front cloud system.

The above analysis indicates that rainfall over inland increases with the eastward movement and development of low vortex, and the location of the rainfall center is consistent with the low vortex center (Figure 1).

Generally speaking, the development process of low vortex precipitation over the Meiyu front is associated with favorable circulation background. The process usually occurs when circulations at high, middle and low levels are in phase with each other.

Based on analysis of rainfall amount every 6 h and wind fields at different levels (not shown), a distinct cyclonic circulation over the Yangtze-Huaihe region at 850 hPa is located where low vortex and rainfall center existed. Therefore, rainfall is closely related to the low vortex circulation which moved northeastward. Trough area exists corresponding to the low vortex at 500 hPa where southeastly and southwestly wind steered by Subtropical High transports warm and moist air flow northward and encounters with northwestly from the north over the Yangtze-Huaihe region. South Asian High occupies the Yangtze-Huaihe region at 200 hPa and the low vortex exists under the divergence field of high level. Thus, the divergence at high level accompanied by the convergence at low level is favorable for the maintenance and development of the low vortex and then provides an advantageous circulation condition for precipitation.

It is obvious that northwestly prevailing over the whole troposphere to the northwest of the low vortex provides cold/dry air for low vortex precipitation.

2 Characteristics of dry intrusion in accompany with low vortex precipitation over Meiyu front

2.1 Characteristics of dry intrusion on satellite vapor cloud image

On satellite vapor cloud image, white and bright areas indicate vapor or cloud cluster while gray and dark areas denote comparatively dry air.

Studies of Browning et al.[2] and Young et al.[8,9] about dry intrusion suggested that vapor cloud image has high temporal resolution and can be easily identified. The vapor cloud image is widely used to reveal the development process of cyclone because it can clearly show the subtle characteristics of cyclone evolution. Roger et al.[29] regard dark area on vapor cloud image as dry air but have not put forward a quantitative index to represent dry air areas.

To better describe the evolution process of dry intrusion using vapor cloud image, the 6.7 μm vapor cloud image from GOES-9 satellite is employed in numerical analysis. According to the formula of equivalent brightness temperature (referred to as brightness temperature hereafter):

Gray Scale Temperature = (255-Gray Scale)×0.5–95 (where Gray Scale ranges from 0 to 255).

Then the possible brightness temperature scale of surface and vapor of cloud (i.e. 32.5—–95.0℃) is divided into 4 scales, i.e. 32.5—–27.0℃ as heavy gray dark area, –27.5—–39.0℃ as gray dark area, –39.5—–51.0℃ as light gray dark area and –51.5—–95.0℃ white bright

area. For vividly depicting vapor cloud image, 84 kinds of gradual changing color are used to denote the color barn of vapor cloud image. And the dark areas with brightness temperature ranging from −15.5℃ to −27.5℃ are representative of dry intrusion.

Here, hourly digital vapor cloud images are only shown at 6 h intervals (Figure 2) to reveal the evolution of dry intrusion for the sake of brevity.

During the period of the formation of low vortex (i.e. 00TC 22 June shown as Figure 2(a)), westly trough at high level exists over the middle reaches of the Yellow River of China near 35°N. Two small dark regions marked by "1" and "2" appear to the south and north of the middle reaches of the Yellow River respectively. On 06UTC 22 June (i.e. initial stage of low votex development, Figure 2(b)), the expanding dark regions "1" and "2" both have larger areas and region "2" moves southeastward. During the middle stage of low votex development (i.e. 06UTC 22 June, Figure 2(c)), dark region "1" moves eastward to 113°E, both regions "1" and "2" develop and intensify. When time goes to 18UTC 22 June (i.e. the mature stage of the low vortex, Figure 2(d)), dark region "1" moves 7—8 longitude eastward, and region "2" extends and intensifies while shifting southeastward. The two dark regions are merging to each other. Next, interactions between the low vortex and dry intrusion symbolized by the above two dark regions lead to the maintenance and eastward movement of the low vortex. During the mature period of low vortex development (after 21UTC 22 June, figure omitted), the low vortex develops into a cyclone and then moves to seas. At the same time, dark regions "1" and "2" connect to one integrated region (shown as Figure 2(e)). It develops and moves eastward with anticlockwise turn-

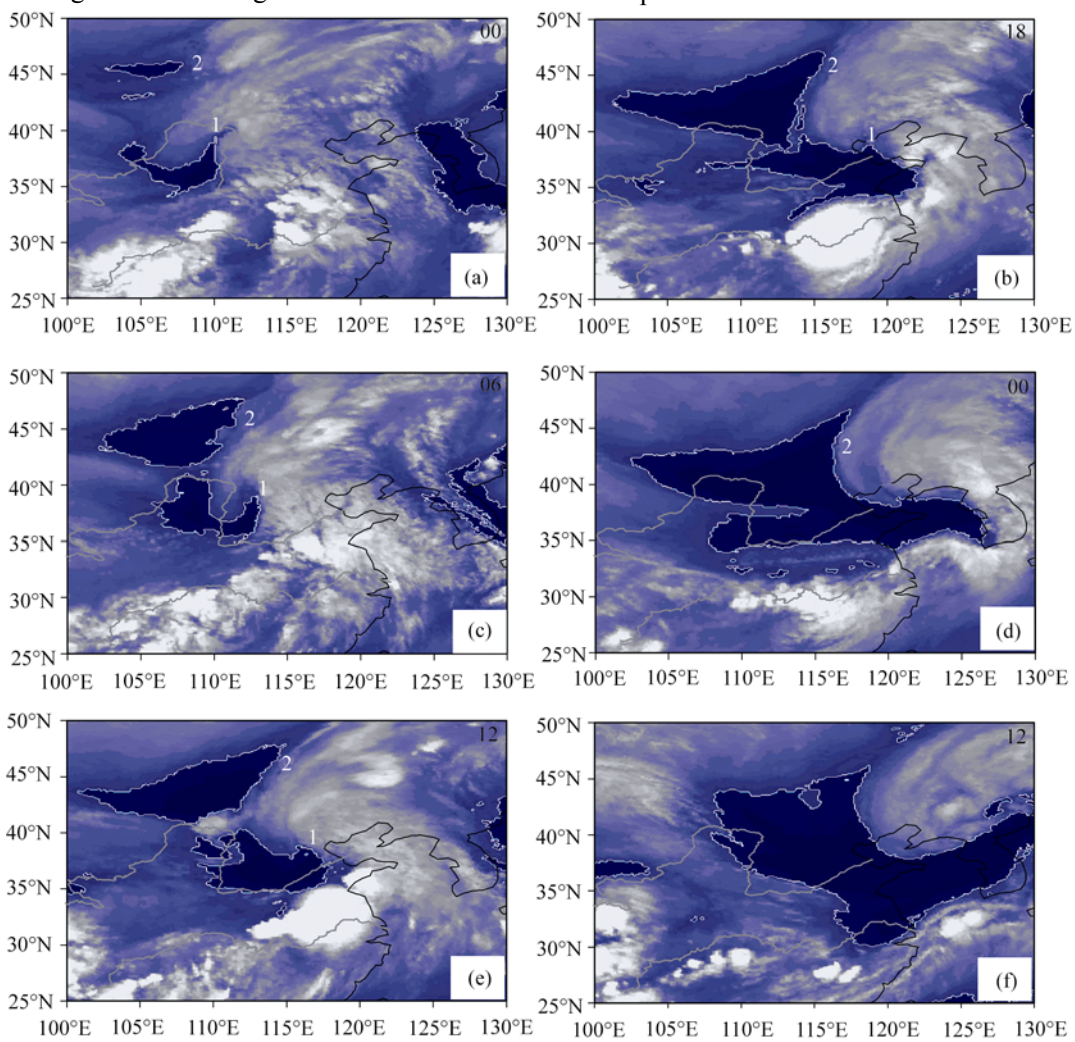

Figure 2 GOES-9 satellite digital vapor cloud images at 6 h intervals during 22 to 23 June in 2003. (a) 00UTC 22 June; (b) 06UTC 22 June; (c) 12UTC 22 June; (d) 18UTC 22 June; (e) 00UTC 23 June; (f) 12UTC 23 June, Dark regions outlined by white solid line denoting dry intrusion; "1" and "2" symbolizing dark regions.

ing up on its front (shown as Figure 2(f)). The dark region appears in semicircle shape on 06UTC 24 June (figure omitted). The cyclone is occluded and then weakens to die out when the dark region constantly besieges it.

In addition, it can be also found that the dark regions expand with southeastward movement during the development of the low vortex from the consecutive track of the dry intrusion (Figure 3).

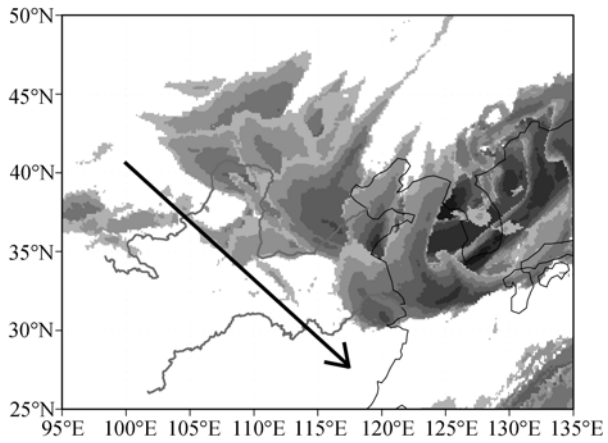

Figure 3 Consecutive track of dry intrusion at 12 h intervals on GOES-9 vapor cloud image for the period of 00UTC 22 June to 00UTC 25 June in 2003. Arrowhead denoting the general direction of the dry intrusion movement.

2.2 Characteristics of dry intrusion on humidity field

As above mentioned, dark regions on vapor cloud image denote dry intrusion. Then how does dry intrusion behave and evolve in humidity fields at different levels?

Based on the description of Browning et al.[2] about dry intrusion, relative humidity (RH) less than 60% is used to represent dry intrusion flow.

From distributions of RH at different levels, dry intrusion flow with RH < 60% always exists to the northwest of low vortex precipitation area. Nevertheless, the intensity and range of low RH vary at different levels. For RH at 300 hPa high level (the right column of Figure 4), one dry area in tongue shape intrudes southeastward under the northwestly steering flow. The RH gradient is the largest in front of the dry area, which is coincident with precipitation. Northwestly flow prevails over dry area during the entire development period of low vortex from the initial stage (Figure 4(d)) to the mature stage (Figure 4(f)). Then the northwestly flow gradually weakens and turns to westly or southwestly wind which steers dry intrusion to cyclonic rotation (not shown). For RH at 500 hPa level (the left column of Figure 4), the distribution and evolution characteristics of dry area are similar to those at 300 hPa. But the scope of dry area at 500 hPa is comparatively larger than that at 300 hPa and the foreside of dry area at 500 hPa exists to the west of that at 300 hPa. For RH at 850 hPa (figure omitted), dry intrusion also occurs to the west of low vortex and moves eastward with the development of low vortex. However, both northwestly and northeastly flow exist over dry area at 850 hPa.

It can be seen from the above analysis that dry intrusion flow can appear at each level of troposphere during the development of low vortex. It is comparatively strong and eastward located at middle and high levels of troposphere. The dry intrusion flow originating from the northwestly flow over middle-high latitudes exerts important effects on the development of low vortex. Precipitation occurs near the region with large RH gradient rather than dry intrusion area at high level. Precipitation also occurs to the west region with large RH gradient at low level, this may be related to the CISK mechanism[30].

By comparing distributions of RH at high level (the right column of Figure 4) with vapor cloud image (Figure 2), it can be found that the distribution area with RH < 60% at high level is analogous with that of dry region on vapor cloud image. However, the distribution of RH cannot reveal the two dry intrusion and their interactions on vapor cloud image. Therefore, the characteristics of dry intrusion can be most clearly described on vapor cloud image.

2.3 Characteristics of dry intrusion on temperature field

Vertical section across low vortex center of potential temperature and meridional wind is shown in Figure 5. The contours of potential temperature bulge upward to the west of low vortex and northerly cold wind prevails in the whole troposphere. Therefore, the dry intrusion has cold property. With the strengthening of northerly wind, the low vortex develops accompanied by increasingly warming near its center and more precipitation.

3 Mechanisms of dry intrusion in accompany with low vortex precipitation over Meiyu front

From the above analysis, dry intrusion coinciding with

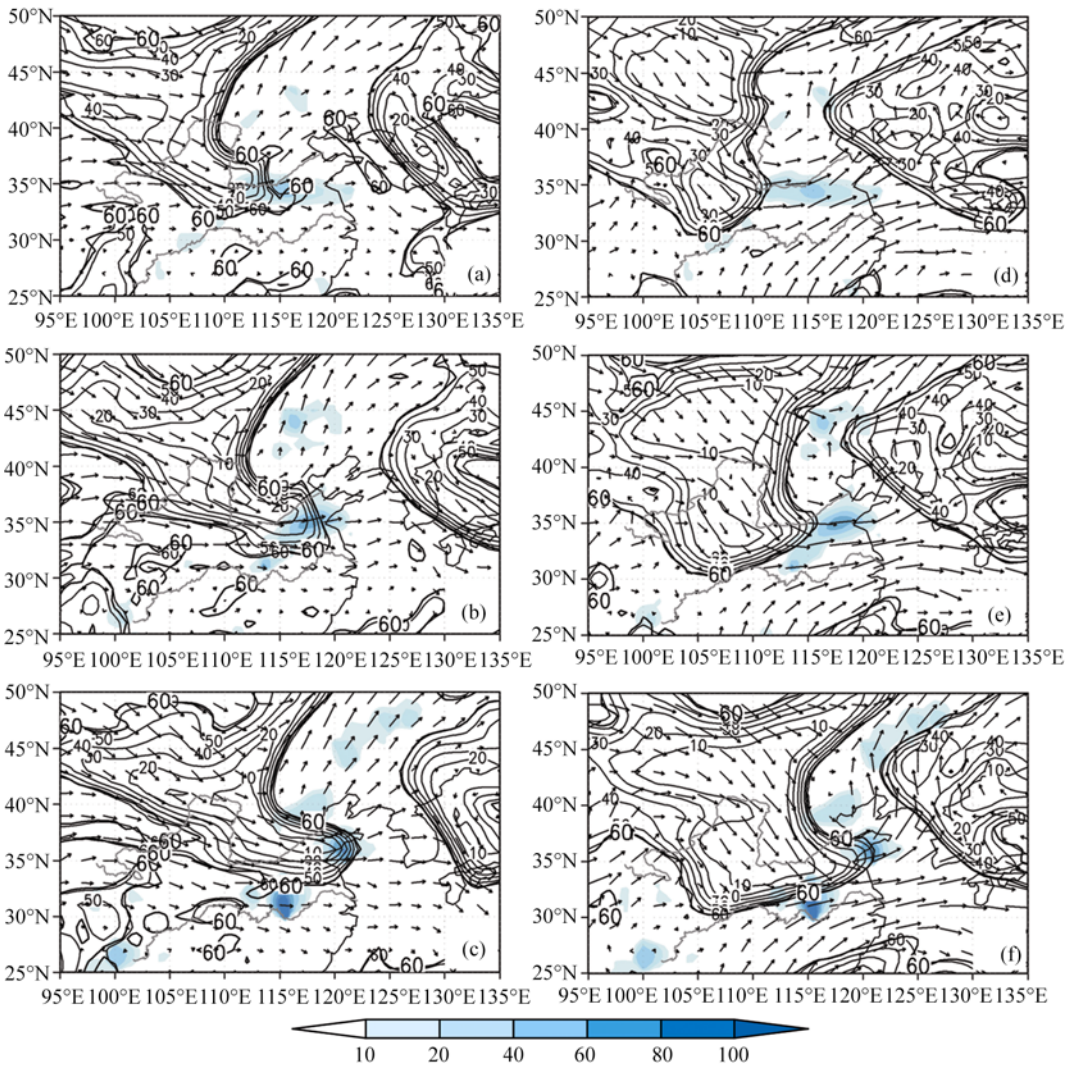

Figure 4 Geographical distribution of RH field (unit: %) superimposed with wind field and 6 h precipitation (shaded areas) at 500 hPa (left column) and 300 hPa (right column) during 22 June of 2003. (a), (d) 06UTC; (b), (e) 12UTC; (c), (f) 18UTC.

low vortex precipitation over the Meiyu front comes from different levels and it is more eastward located and stronger with the increasing height. Then, what is the mechanism of dry intrusion?

Figure 6 shows vapor cloud image, PV, pressure and wind on 345 K isentropic surfaces during 22 June of 2003. The isentropic surface near 40°N−25°N looks like a special "bowl"(dashed line), on the west of which a gap exists. There is a zonal region with comparatively large pressure gradient. The isentropic surface is the most abrupt over the zonal region, on the west of which northerly wind prevails. With the eastward intrusion of northerly wind, precipitation region continuously expands and shifts eastward. Precipitation always occurs at the bottom of the "bowl", where divergence exists between southwesterly wind and southerly wind. In addition, the southwesterly wind flowing along the wall of the "bowl" makes the isentropic surface more abrupt (18UTC 22 June shown as Figure 6(c)).

The configuration of isobaric lines and wind on isentropic surface can reflect cold or warm advection since the former are equivalent to isothermohyps on isobaric surface. In frictionless and adiabatic motion, PV is conserved on isentropic surface according to Hoskins' description about PV[31]. The dense ribbon of PV on isentropic surface denotes the location of tropopause which is also the folding belt on tropopause.

Cold advection to the north of the folding belt and regular southeastward movement of high PV air currents can also be seen from Figure 6. Cold advection controls the front of high PV while warm advection controls the east of high PV region. The southward intrusion of cold

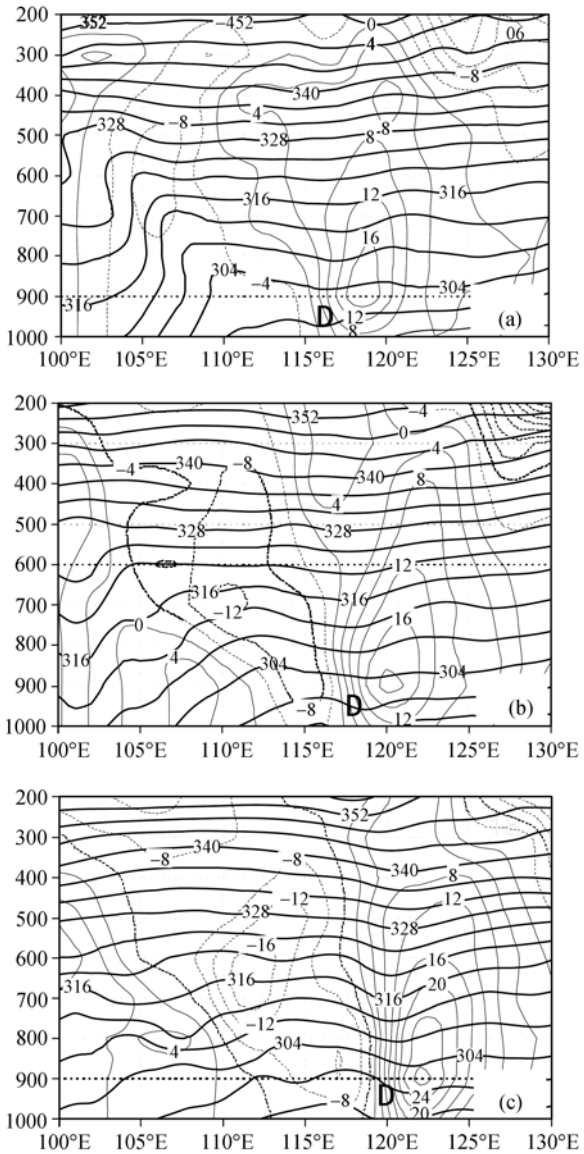

Figure 5 Vertical section across low vortex center for potential temperature (K, thick lines) and meridional wind (m/s, thin lines) during 22 June of 2003. (a) Along 34°N on 06UTC; (b) along 35°N on 12UTC; (c) along 36°N on 18UTC. Thin solid/dashed lines denoting south/north wind; D symbolizing low vortex center.

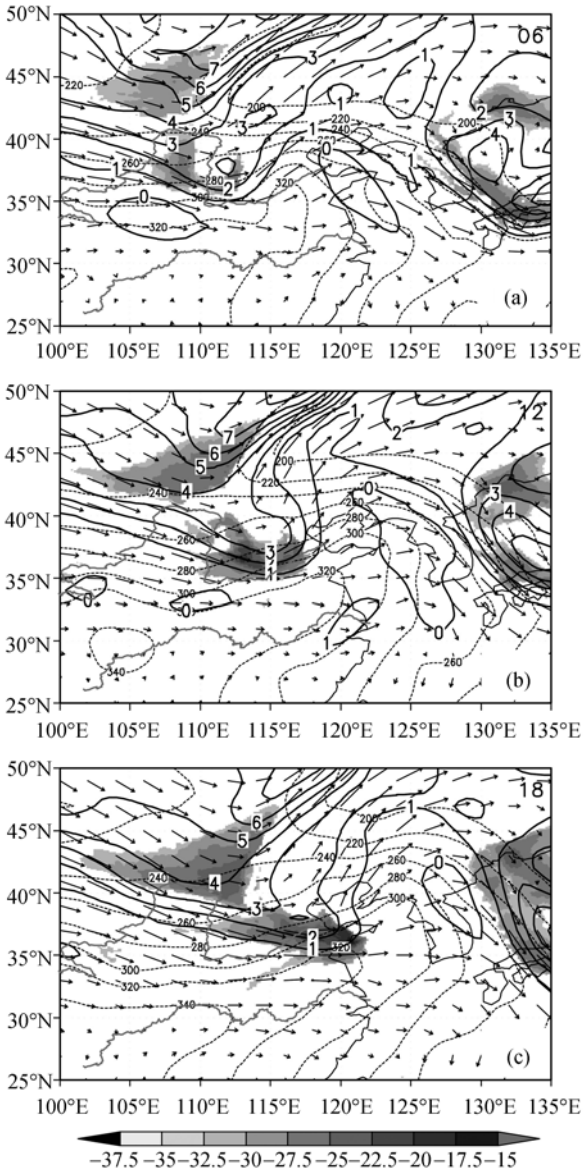

Figure 6 Overlap of vapor cloud image (shaded areas), PV (PVU, solided lines), pressure (hPa, dashed lines) and wind on 345K isentropic surface during 22 June of 2003. (a) 06UTC; (b) 12UTC; (c) 18UTC.

advection is favorable for the development of low vortex. Cold air at high level descends under the cold advection to the west of low vortex. Although descending motion leads to warming, the isentropic surface bulges upward and temperature is comparatively low to the west of low vortex because of the strong cold advection (Figure 5). As a result, the low vortex intensifies and rainfall increases under the impacts of descending motion and cold advection to the west of the low vortex.

It can also be found that dry intrusion areas represented by digital vapor image (shaded area in Figure 6) correspond well to high PV on isentropic surface and the front of dry intrusion is consistent with dense ribbon of PV contours. With the development and eastward shifting, dry intrusion and high PV air flows move southeastward concurrently under the northwesterly steering flow. The mechanism of dry intrusion can be considered as the intrusion and downward spread of high PV. Dry intrusion can be regarded as one important index of the intrusion of high PV on the other hand.

In addition, high PV descends from high level to low level along isentropic surface to the west of low vortex and the west of 35°N. Based on the theory of down-

sliding PV development[16], vertical PV develops at middle and low levels and low vortex intensifies when dry intrusion flow with high PV descends from high level along isentropic surface. The same case occurs when warm and moist flow ascends along isotropic surface over the east of low vortex[32].

4 3-D structure of dry intrusion and its impacts on low vortex precipitation

4.1 3-D structure of dry intrusion

Recent studies show that dry intrusion exerts important effects on heavy rainfall during the Meiyu period. Four dry intrusion processes occurred corresponding to 4 heavy rainfall processes during the Meiyu period in 2003. Heavy rainfall intensifies during the gradual development of dry intrusion because dry intrusion leads to the formation and maintenance of dry level which reduces temperature and humidity[28].

Next, isentropic analysis is used to clearly identify the 3-D structure of dry intrusion and intuitionally reveal the evolution and characteristics of dry intrusion.

Based on analysis of RH, height, wind and 6 h rainfall amount on 320 K and 345 K isentropic surfaces (Figure 7), dry area with RH less than 60% can reach the Yangtze-Huaihe region and low vortex precipitation occurs in front of the dry area. Figure 7 shows the height of descending and eastward movement of dry area. It suggests that the front of area with RH less than 60% on 345 isentropic surface is more eastward located than that on 320 K one.

During the development of low vortex, dry intrusion

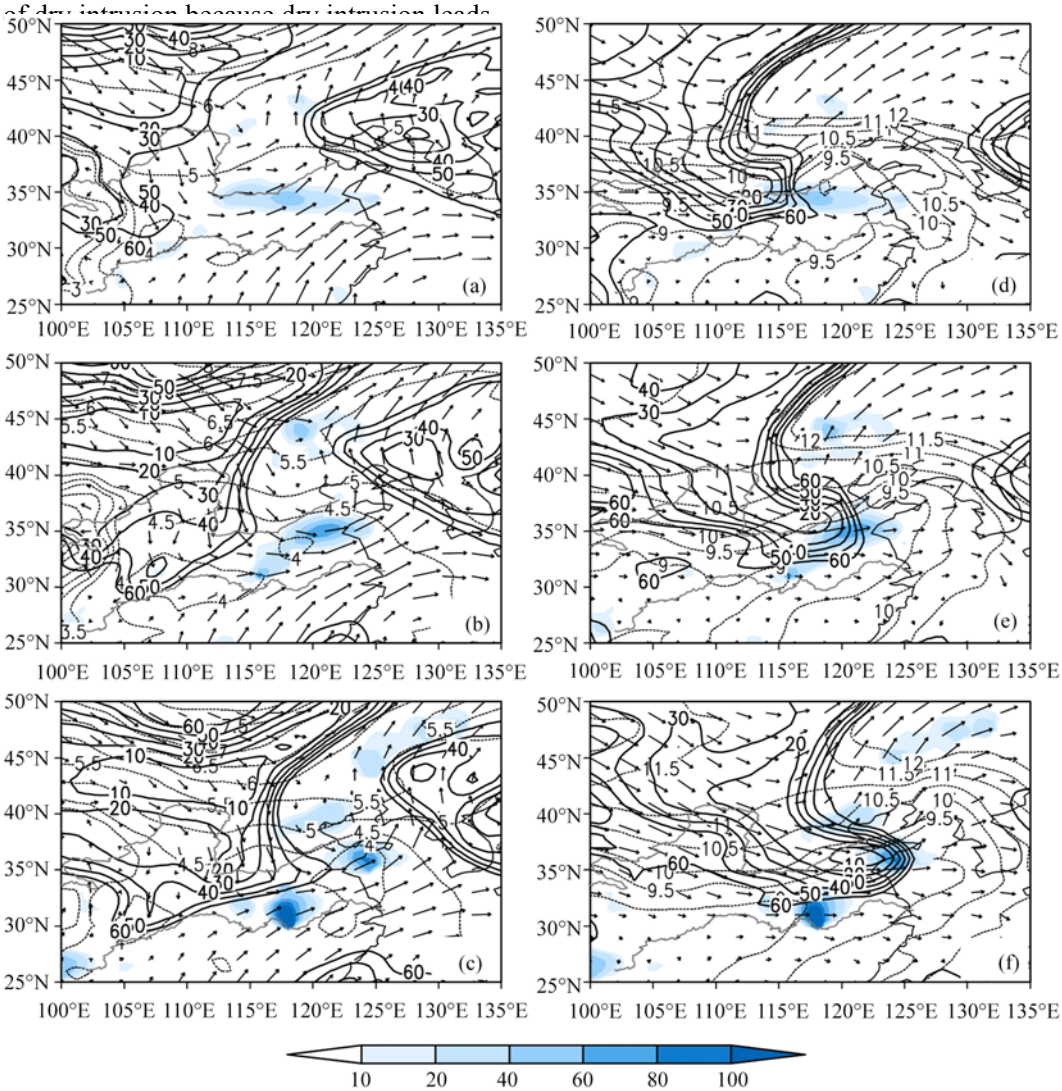

Figure 7 Overlap of RH (%, solided lines), height (km, dashed lines), wind and 6 h precipitation (mm,shaded areas) on 320 K (left column) and 345K (right column) isentropic surfaces during 22 June of 2003. (a), (d) 06UTC; (b), (e) 12 UTC; (c), (f) 18UTC.

intrude from 8 km height to 4 km along 50°N under the control of northerly or northwesterly steering wind on 320 K isentropic surface (left column of Figure 7). For the initial stage of low vortex development, the front of isograms with RH equal 60% moves eastward from 110°E on 06UTC 22 June (shown as Figure 7(a)) to 115°E on 12UTC 22 June (shown as Figure 7(b)), and then to 120°E on 18UTC 22 June (shown as Figure 7(c)). Rainfall occurs over the moist side of the front of dense belt of RH isograms. Low vortex and accompanied precipitation intensify and move eastward with the eastward shift of dry areas. On the other hand, dry intrusion intrudes from 11.5 km height to 9 km under the control of northerly or northwesterly steering wind on 345 K isentropic surface (right column of Figure 7); rainfall occurs over the dense belt of RH isograms. Low vortex precipitation also moves eastward with the eastward shift of dry areas.

Therefore, dry intrusion glides along isentropic and its evolution on different isentropic surfaces are closely associated with the location of precipitation.

4.2 Impacts of dry intrusion on low vortex precipitation

(i) Enhancement effect of dry intrusion on convective instability of low vortex precipitation areas. According to the characteristics of RH field on isentropic surfaces, dry areas can clearly reveal the activities of dry intrusion in 3-D space. It can be seen from distributions of dry intrusion on different isentropic surfaces (Figure 7) that the dry intrusion at high level is situated more eastward than that at lower level.

The intensity of dry intrusion over low vortex varies from different heights. Thus, dry stratification at high levels and moist stratification at lower levels leads to $\frac{\partial \theta_{se}}{\partial z} < 0$ because low vortex at lower levels is below dry/cold advection at higher levels. Correspondingly, the convective instability develops; cyclonic circulation of low vortex enhances and low vortex precipitation increases. Dry intrusions with different strength intrude into different heights over the west side of low vortex, resulting in cold advection to different degree at different levels over the low vortex precipitation region. Then the increscent vertical temperature difference makes convective instability over low vortex precipitation develop, which has enhancement impacts on heavy rainfall.

In brief, the cooling and dryness effects of dry intrusion on low vortex precipitation system do contribute to the enhancement of convective instability and the corresponding increase of low vortex precipitation.

(ii) Enhancement effect of vertical overlap of high PV perturbation on low vortex precipitation. Vertical gradient of potential temperature decreases with the reduction of height. Its vertical gradient is comparatively large near tropopause. In frictionless and adiabatic motion PV is conserved on isentropic surface[15], i.e. $PV = \alpha \zeta_\theta |\nabla \theta|$. Absolute vorticity increases when $|\nabla \theta|$ decreases because of the descent of dry intrusion. Low vortex develops and rainfall increases under the circumstances.

Isentropic coordinate (i.e. θ coordinate) is used here to better display the 3-D structure of low vortex system and the characteristics of vertical overlap of PV on different isentropic surfaces.

Figure 8 shows many kinds of physical elements in vertical section along low vortex center in θ coordinate. For the initial stage of low vortex development (06UTC 22 June, shown as Figure 8(a)), one positive PV region with center value of 1.5PVU exists on 320 K isentropic surface while the region with high PV larger than 1.0PVU exists over 350 K isentropic surface. High PV region over the Yangtze-Huaihe region on 320 K isentropic surface is corresponding to low vortex precipitation region. Westly wind prevails and descent motion is not so clear over the west of low vortex. During the middle stage of low vortex development (12UTC 22 June, shown as Figure 8(b)) on 320 K isentropic surface (i.e. high level), high PV intensifies to the west of low vortex near 115°E and the westerly wind descending through isobaric surfaces transports high PV from high level to the east. The high PV near 118°E at lower level extends to high level and surface layer. Thereinto, 1PVU and 1.5PVU centers emerge on 345 K isentropic surface and surface layer respectively. So the downward transport of high PV and the emergence of high PV at surface layer contribute to the development of low vortex and the increase of precipitation. For the mature stage of low vortex development (18UTC 22 June, shown as in Figure 8(c)), high PV region gets through the high, middle and low levels. Isograms with 1PVU reaches 300 K isentropic surface. High PV region with PV larger than 1.5PVU distinctly expands along 120°E on 320 K isentropic surface and triggers effects on the wind field with maximum cyclonic curvature and the maintenance of

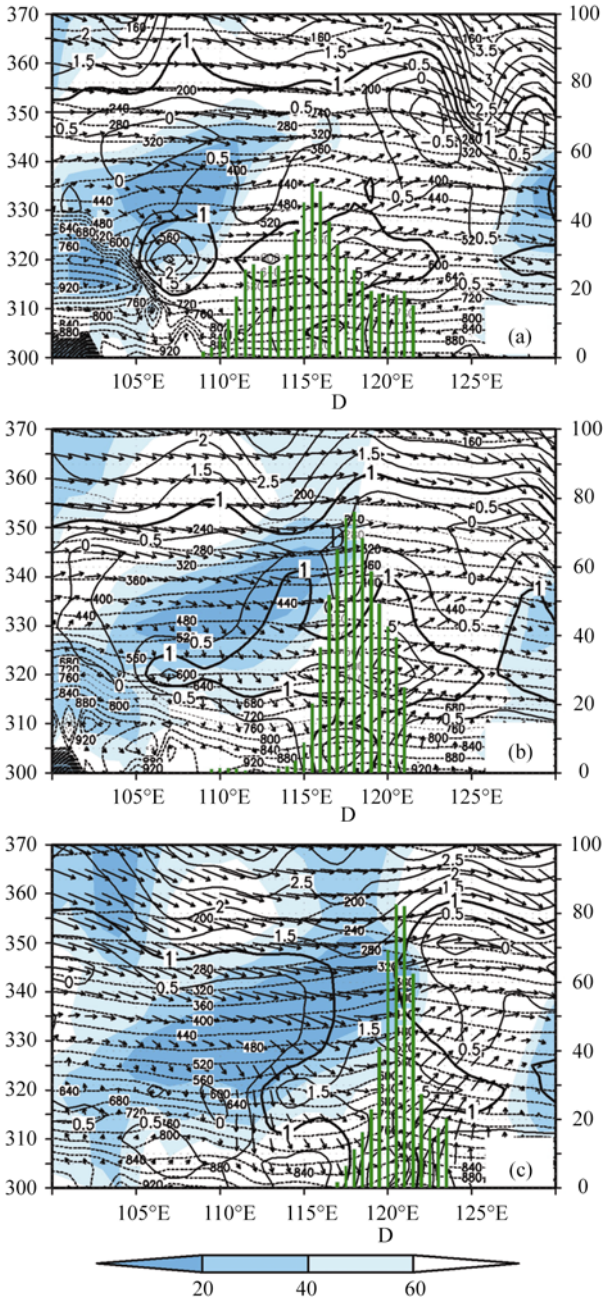

Figure 8 Vertical section across low vortex center for PV (PVU, solided lines; thick solided line denoting 1PVU isograms), pressure (hPa, dashed lines), RH (%, shaded areas denoting RH less than 60%), wind and 6 h precipitation (mm) on isotropic coordinate during 22 June of 2003. (a) 06UTC; (b) 12UTC; (c) 18UTC.

rainfall. Therefore, low vortex precipitation is corresponding to the perturbation of high PV. The strengthening of flow descending through isobaric surfaces to the west of low vortex precipitation leads to the downward transport of high PV from high level. The downward transport of high PV from high level and the corresponding increase of PV at middle and low levels are in favor of the development of low vortex and the increase of rainfall. On the other hand, the latent heat of condensation released by low vortex precipitation in turn bring about the increase of PV at middle and low levels which is in favor of the development of low vortex under the joint effects of high PV at high and low levels.

It can also be seen from Figure 8 that dry areas (shaded areas in Figure 8) with RH less than 60% exist to the west of low vortex during the eastward development of low vortex precipitation. The strongest dry area is situated on 330 K isentropic surface. Dry areas expand, strengthen and move eastward with the increase and eastward shift of low vortex precipitation. According to the configuration between low vortex precipitation region and dry areas with RH less than 60%, dry intrusion distinctly leans eastward with the decreasing height of isentropic surface. The characteristics of dry intrusion may be one of the important factors resulting in the development of convective instability over low vortex precipitation.

Therefore, the vertical overlap of high PV perturbation favors the development and maintenance of low vortex precipitation. The cold advection from high levels transported by westerly wind descending through isobaric surfaces to the west of low vortex region will set off the formation and development of convective instability. The significant eastward inclination of dry intrusion with the increasing height of isentropic surface is in favor of the development of instability over low vortex precipitation.

5 Conclusions

Characteristics of dry intrusion accompany low vortex precipitation over the Meiyu front on satellite vapor cloud image, relative humidity field and isentropic surfaces are analyzed in this paper. Mechanism of dry intrusion and its effects on low vortex precipitation are also discussed. The following conclusions can be drawn:

(1) The formation, development and maintenance of low vortex over the Meiyu front are closely related to the evolution of dry intrusion. The dry intrusion has characteristics of high PV, low relative humidity and low temperature.

(2) Dry intrusion appears as dark areas on 6.7 μm vapor cloud image and areas with RH less than 60% in RH field. But the vapor image can give comparatively vivid depiction of dry intrusion. The digital vapor image

with high spatial and temporal resolution vividly reveals characteristics of the development, evolution and interaction of dry intrusion during the evolvement of low vortex. Therefore, digital vapor image can serve as good tools for studying dry intrusion.

(3) Dry intrusion comes from different levels of troposphere and it declines eastward with increasing height. The cold advection resulting from eastward declining dry intrusion and descendent motion through isentropic surfaces are favorable for the development of convective instability over low vortex and the corresponding increase of low vortex precipitation.

(4) Dry intrusion is in step with PV perturbation at high levels. They both moves southeastward under northwesterly steering flow with the eastward development of low vortex. The mechanism of dry intrusion is the downward transportation and intrusion of high PV. Dry intrusion is one important index of the intrusion of high PV. The dry intrusion on vapor cloud image is the most vivid description about forcing effects of downward transporting high PV at lower level. It can be used in weather prediction.

(5) Analysis about characteristics on isentropic surfaces and θ coordinate can be adopted to demonstrate the 3-D structure of dry intrusion. Dry intrusion from high level always intrudes along isentropic surfaces into lower level near low vortex. The configurations between low vortex precipitation region and the front of dry intrusion vary with heights.

It should be noticed that the case study in this paper mainly aims at the low vortex precipitation over the Yangtze-Huaihe region during the Meiyu period. Dry intrusion of this case may appear more evident than that over the Yangtze River and regions to its south. At the same time, the case study about effects of dry intrusion on low vortex precipitation should be validated by more cases or model tests.

1 Tao S Y. Heavy Rainfall in China (in Chinese). Beijing: Science Press, 1980. 1－225
2 Browning K A, Golding B W. Mesoscale aspect of a dry intrusion within a vigorous cyclone. Q J R Meteorol Soc, 1995, 121(523): 465－493
3 Danielsen E F. Project Springfield Report. Defense Atomic Support Agency, Washington D. C. 20301, DASA 1517(NTIS#AD – 607980), 1964, 1－97
4 Browning K A, Roberts N M. Structure of a frontal cyclone. Q R J Meteorol Soc, 1994,120 (520): 1535－1557
5 Browning K A. The dry intrusion perspective of extra-tropical cyclone development. Meteorol Appl, 1997, 4(4): 317－324 [DOI]
6 Browning K A, Roberts N M. Variation of frontal and precipitation structure along a cold front. Q J R Meteorol Soc, 1996, 122(536): 1845－1872 [DOI]
7 Young M V. A classification scheme for cyclone life-cycles : Applications in analysis and short-period forecasting. The life cycles of extratropical cyclones, Vol. 3. Proceedings of an International Symposium, 27 June－1 July 1994, Bergen, Norway
8 Young M V. Extratropical cyclones-a forecaster's perspective. Meteor Appl, 1997, 4(4): 293－300 [DOI]
9 Young M V, Monk G. A, Browning K A. Interpretation of satellite imagery of a rapidly deepening cyclone. Q J R Meteorol Soc, 1987, 113(478): 1089－1115 [DOI]
10 McCallum E, Clark G V. Use of satellite imagery in a marked cyclogenesis on 12 November 1991. Weather, 1992, 47: 241－246
11 Leslie R L. On the mesocyclone"dry intrusion" and tornadogesis, preprints, 19th. Conf. on Sever Local Storm, Minneapolis, Amer Meteor Soc, 1998, 752－755
12 Yu Y B, Yao X P. Reviews on t he dry intrusion and its application. Acta Meteor Sin (in Chinese), 2003, 61(6): 669－778
13 Ninomiya K, Muraki H. Large-scale circulation over east Asia during Baiu period of 1979. J Meteor Soc Japan, 1986, 64(3): 429－409
14 Ninomiya K. Large and meso-α-scale characteristics of Meiyu/Baiu front associated with intense rainfalls in 1－10 July 1991. J Meteor Soc Japan, 2000, 78(2): 141－157
15 Wu G X, Liu H Z. Complete form of vertical vorticity tendency equation and slantwise vorticity development. Acta Meteor Sin (in Chinese), 1999, 57(1): 1－15
16 Wu G X, Cai Y P, Tang X J. Moist potential vorticity and slantwise vorticity development. Acta Meteor Sin (in Chinese), 1995, 53(4): 387－405
17 Lu E, Ding Y H, Li Y H. Isentropic potential vorticity analysis and cold air activity during the period of excessively heavy rainfall over Changjiang-Huaihe River Basin in 1991. J Appl Meteor Sci (in Chinese), 1994, 5(3): 19－27
18 Yu Y B, Yao X P. The diagnosis analysis of potential vorticity for a typhoon heavy rainfall in North China. Plateau Meteorol (in Chinese), 2000, 19(1): 111－120
19 Jiang J Y, Ni Y Q. Diagnostic study on the structural characteristics of a typical Mei-yu front system and its maintenance mechanism. Adv Atmos Sci, 2004, 21(5): 802－813
20 Huang W, Tao Z Y. Analysis of cold air activity during Meiyu period in 1991. Chin J Atmos Sci (in Chinese), 1995, 19(3): 375－379
21 Yuan J S, Shou S W. Potential vorticity analysis in cold air activities during the south China torrential rain in 1998. J Nanjing Inst Meteorol (in Chinese), 2001, 24(1): 92－98
22 Shou S W, Li Y H, Fan K. Diagnostic analyses of development of mesoscale cyclone during torrential rain. Acta Meteor Sin (in Chinese), 2001, 59(6): 560－568
23 Gao K, Xu Y M. A simulation study of structure of mesovortexes along Meiyu f ront during 22－30 June 1999. Chin J Atmos Sci (in Chinese),

2001, 25(6): 740－756
24 Rogers E, Bosart L F. An investigation of explosively deepening oceanic cyclones. Mon Wea Rev, 1986, 114: 702－718 [DOI]
25 Lǔ M, Lu H C, Diagnostic analysis of cyclone development over Changjiang-Huaihe River Basin in spring. J Meteorol Sci (in Chinese), 1997, 17(1): 10－16
26 Davis, C A, Emanuel K A. Potential vorticity diagnostics of cyclogenesis. Mon Wea Rev, 1991, 119(8): 1929－1953 [DOI]
27 Rossa A M, Wernli H, Davies H C. Growth and decay of an Extro-tropical cyclone's tower. Meteorol Atmos Phys, 2003, 73: 139－156 [DOI]
28 Yao X P, Yu Y B. Activity of dry cold air and its impacts on Meiyu rain during 2003 Meiyu period. Chin J Atmos Sci (in Chinese), 2005, 29(5): 973－985
29 Roger B W, Susan J H. Description and Application of Vapor Cloud Images on Weather Analysis and Prediction (Translated Zheng X J, et al.) (in Chinese). Beijing: Metrological Press, 1994. 60－64
30 Hu B W. The band of CISK coupled with low level "moisture fronts" and the genesis of warm shear line-type Meiyu fronts. Chin J Atmes Sci (in Chinese), 1997, 21(6): 679－686
31 Hoskins B J, Mclntyre M E, Robertson A W. On the use and significance of isentropic potential vorticity maps. Q J Roy Meteor Soc, 1985, 111: 877－946 [DOI]
32 Cui X P, Wu G X, Gao S T. Numerical simulation and isentropic analysis of frontal cyclones over the western Atlantic ocean. Acta Meteor Sin (in Chinese), 2002, 60(4): 385－398